

Brownian motion of optically anisotropic particles in weak polymer gels

P. Díaz-Leyva, E. Pérez, and J.L. Arauz-Lara
*Instituto de Física “Manuel Sandoval Vallarta”,
 Universidad Autónoma de San Luis Potosí, Álvaro Obregón
 64, 78000 San Luis Potosí, S.L.P., Mexico*

Recibido el 29 de junio de 2004; aceptado el 3 de agosto de 2004

The translational and rotational dynamics of optically anisotropic colloidal particles in viscoelastic polymer gels is studied by dynamic light scattering. Polymer gels are formed by polymerization of acrylamide and bis-acrylamide, as cross-linking agent, in water. Particles with crystalline internal structure are made by emulsification of liquid crystal at the nematic phase and a further consolidation. In this work we consider only low fractions of cross-linking, where the systems are ergodic and gaussian statistics is valid. Experimental results for the rotational and translational mean squared displacements, showing the effect of the system's viscoelasticity on both diffusion modes, can be fitted to an extended model of Brownian particles harmonically bounded to a multicomponent of weak elastic restoring forces.

Keywords: Dynamic light scattering; rotational diffusion; gels.

La dinámica traslacional y rotacional de partículas coloidales ópticamente anisotrópicas en geles de polímeros son estudiadas por dispersión dinámica de luz. Los geles de polímero están formados con acrilamida y bis-acrilamida, como agente entrecruzador en agua. Las partículas con estructura cristalina interna están hechas emulsificando un cristal líquido en su fase nemática y posteriormente consolidándolo. En este trabajo consideramos únicamente geles a una baja fracción de agente entrecruzador, en donde los sistemas son ergódicos y la estadística gaussiana es válida. Los resultados experimentales para el desplazamiento cuadrático medio traslacional y rotacional, que muestrean el efecto viscoelástico de estos sistemas en ambos modos, pueden ser ajustados a un modelo extendido de una partícula browniana armónicamente ligada a un multicomponente de fuerzas elásticas restauradoras débiles.

Descriptores: Dispersión dinámica de luz; difusión rotacional; geles.

PACS: 82.70.Gg; 82.70.Dd; 05.40.Jc

1. Introduction

The diffusion of colloidal tracers in complex fluid media, such as polymer solutions, cells, microemulsions, colloidal suspensions, etc, has been largely used to determine different properties of these systems: permeability, bicontinuity, particle grow, etc. In a simple viscous fluid, the motion of a tracer is described by the mean squared displacement $W(t) \equiv \langle [\mathbf{r}(t) - \mathbf{r}(0)]^2 \rangle / 6$, where $\mathbf{r}(t)$ is the position of the tracer particle at time t , and the angular parenthesis indicate the equilibrium ensemble average. For non-interacting particles (*i.e.*, in the limit of infinite dilution of the tracer particles) in an homogeneous system, $W(t)$ is a linear function of time, *i.e.*,

$$W(t) = Dt, \quad (1)$$

in the diffusive time regime, defined by $t \gg \tau_B \equiv m/\zeta$, where m and ζ are the particle's mass and the translational friction coefficient, respectively [1]. The slope D of the mean squared displacement is the free-particle self-diffusion coefficient given by the Einstein relation, $D = k_B T / \zeta$, where $k_B T$ is the thermal energy. For a spherical particle of diameter σ with stick boundary conditions, the friction coefficient is $\zeta = 3\pi\eta\sigma$, with η being the shear viscosity of the solvent. In the absence of interactions with neighbour particles and external fields, deviations from Eq. (1), reflect the complexity of the local mechanical properties of the host medium. Thus, random motion of tracer particles probes properties of the host fluid, in time and space scales characteristic of the

Brownian motion, *i.e.*, in the submillisecond and submicron ranges, respectively, which are inaccessible to standard mechanical methods [2]. Besides the translational diffusion, due to the fluctuating forces exerted by the fluid on the particles, the particles also rotate randomly due to fluctuating torques exerted by the medium. Thus, rotational motion is analogous to translation and it is described, for small angular displacements $\Delta\theta(t)$ of the particles director, by the mean squared angular displacement $\Omega(t) \equiv \langle [\Delta\theta(t)]^2 \rangle / 4$. For freely rotating spherical particles,

$$\Omega(t) = \Theta t, \quad (2)$$

where $\Theta = k_B T / \pi\eta\sigma^3$ is the rotational diffusion coefficient [3]. Here again, deviations from Eq. (2) are due to the complexity of the medium. So far, most of the work on colloidal diffusion has been devoted to study the translational diffusion, and its relation to local rheological properties of the host [4–8]. However, rotational diffusion is also an interesting dynamical property, which can also be used as an alternative tool to characterize the local properties of system, where the translational motion of the probes is restricted, for instances in porous media.

Here we study the translational and rotational diffusion of optical anisotropic spherical particles in weak gels of cross-linked polyacrylamide in water. The amount of cross-linkers is kept low to insure ergodicity of the system. We use depolarized dynamic light scattering to measure the dynamics, both translational and rotational of the particles for different

cross-linking conditions. As we show below, these systems have viscoelastic properties which are expressed in the behavior of both diffusion modes. The presentation of the work is as follows: in Sec. 2 we describe the preparation of the anisotropic particles and the cross-linked gels. In Sec. 3 we discuss briefly our light scattering setup. In Sec. 4 we present and discuss our results.

2. Sample preparation

2.1. Liquid crystal particles (LCP)

Optical anisotropic spherical colloidal particles were made as follow [9]: 0.2 mg of reactive monomer RM257 (Merck), and 0.1 mg of photo-initiator Darocur 1173 (Ciba) were dissolved in 20 g of ethanol at room temperature. The mixture is then injected into stirring water, producing a poly-disperse dispersion of liquid crystalline (mixed with photo-initiator) droplets in water. The system is allowed to equilibrate at 80°C, above the temperature of the crystal-nematic phase transition of the monomer. The photo-initiator is activated by irradiation with UV light, which polymerizes the monomer, freezing the internal nematic order in the droplet. Suspensions of the anisotropic particles with low polydispersity are obtained by fractionation following Bibette's depletion crystallization method [10]. In the present work, we used particles of hydrodynamic diameter of 340 nm, which are the most abundant species in the batch, with a polydispersity size of 7.25%. In order to illustrate the optical anisotropy of the particles produced by this method, optical microscope images of a liquid crystal particle (LCP) of diameter $\sim 4.0 \mu\text{m}$ suspended in water, observed between two linear polarizers, are shown in Fig. 1. Due to its large size, this particle rotates slowly, and one can follow its rotational motion in detail by optical microscopy. Fig. 1(a) shows the particle when the illuminating and collecting polarizers are parallel. Here, one can see an homogeneous spherical particle. Figs. 1(b)-(d) show images taken at intervals of 4 s, when the polarizers are crossed. These are images of the light depolarized by the particle at different angles between the particle director and the polarization of the incident light, showing the characteristics of the particle internal structure. The particles used in the present work, which are about one order of magnitude smaller than the one used in Fig. 1, also show a strong light depolarization effect. For particles of this size, depolarized light scattering is a better suited experimental technique to study its motion.

2.2. Polyacrylamide gels

Polyacrylamide gels are prepared by polymerizing acrylamide (AA) and bisacrylamide (BA) using ammonium persulfate and tetramethylethylenediamine (TEMED) as initiator and catalyst (Sigma-Aldrich, USA), respectively. BA monomers cross-link polymer chains during polymerization

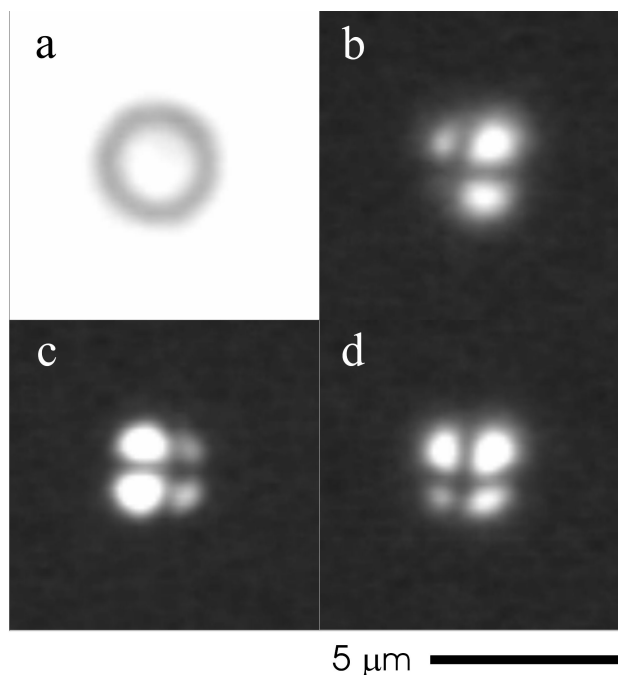


FIGURE 1. Optical anisotropic colloidal particle of diameter $\sim 4 \mu\text{m}$, as seen between two linear polarizers by optical microscopy. The particle is suspended in water. In picture (a) both polarizers are parallel. In (b) to (d) the polarizers are crossed.

process. Thus, the extent of cross-linking depends on the fraction $f_{bis} \equiv [BA]/([AA] + [BA])$. In the present work, f_{bis} was varied in the range from 0.0 to 0.0125, keeping constant the total amount of monomer at 2.5% w/w, i.e., $[AA] + [BA] = 2.5\%$ w/w in all samples. LC particles were dispersed in the monomer solution prior to polymerization which was carried out at room temperature directly in the cuvettes for light scattering; the particle volume fraction was around 10^{-5} . Samples were used 48 hours after preparation. The range of values of f_{bis} used here is kept below the sol-gel transition [11].

3. Light scattering

In this section, we describe the experimental setup and introduce the quantities measured in our light scattering experiments. The setup is standard. The sample is placed in a goniometer (Brookhaven) in the center of an optical vat filled with index matching fluid (decalin). A polarized laser beam of $\lambda = 488 \text{ nm}$ wavelength is focused onto the sample cell. The direction of the x and z axis of the laboratory-fixed frame are defined by the direction of the wavevector of the incident light \mathbf{k}_i , and by the direction of its polarization \mathbf{n} , respectively. The light scattered at the angle θ_s with respect to the axis x is collected by a monomode optical fiber located on the $x - y$ (scattering) plane. A second polarizer is located before the optical fiber to insure that only one mode reaches the detector. The scattered light is split and directed to two photon detectors (ALV/SO-SIPD), and the signal is processed by a time correlator (ALV 6010/160) operated in the pseudo-

cross correlation mode. For ergodic systems, which is the case studied here, the output of the correlator is $g^{(2)}(k, t)$, the ensemble-average of the time correlation function of the scattered light intensity $I(k, t)$, *i.e.*,

$$g^{(2)}(k, t) \equiv \langle I(k, 0)I(k, t) \rangle / \langle I^2(k, 0) \rangle, \quad (3)$$

where $k = (4\pi n_s / \lambda) \sin(\theta_s / 2)$ is the scattering wavevector, and n_s is the refraction index of the medium. The dynamics of isotropic particles can be obtained via the Siegert relation, *i.e.*,

$$g^{(2)}(k, t) = 1 + b |g^{(1)}(k, t)|^2, \quad (4)$$

where $g^{(1)}(k, t)$ is the correlation function of the scattered electric field $\vec{E}(k, t)$ of the wavevector k which describes the translational dynamics of the probes. Eq. (4) is derived assuming the scattered electric field $\vec{E}(k, t)$ to be a complex Gaussian variable [12]. In Eq. (4), b is an experimental constant of order 1 and

$$g^{(1)}(k, t) \equiv \langle \vec{E}^*(k, 0)\vec{E}(k, t) \rangle / \langle |\vec{E}(k, 0)|^2 \rangle. \quad (5)$$

3.1. Isotropic particles

In the case of isolated isotropic probe particles one can use the Siegert relation, Eq. (4), to get $g^{(1)}(k, t)$ from the measured $g^{(2)}(k, t)$. Furthermore, for monodisperse rigid particles the translational mode is the only contribution to the correlation function $g^{(1)}(k, t)$. For freely diffusing particles it is given by

$$g^{(1)}(k, t) = \exp(-k^2Dt), \quad (6)$$

where D is the translational free diffusion coefficient.

3.2. Anisotropic particles

The nematic-like internal structure of the optical anisotropic LC particles, allows us to assume a cylindrical symmetry of the polarizability tensor α with diagonal components α_{\parallel} , α_{\perp} , and α_{\perp} in the particle-fixed frame with the x component pointing in the direction of the particle director $\hat{n}(t)$, a unit vector whose direction, as seen from the laboratory-fixed frame, changes randomly due to fluctuating torques exerted by the solvent molecules. The anisotropy of the scattering particles depolarizes the incident light, and the scattered electrical field can be decomposed in the parallel $E_{VV}(k, t)$, and perpendicular $E_{VH}(k, t)$ components, with respect to the direction of the incident polarization. These quantities fluctuate due to the random translational and rotational motion of the particles, and one can define two different correlation functions between these components of the scattered electrical field, namely,

$$g_{VV}^{(1)}(k, t) = \langle E_{VV}^*(k, 0)E_{VV}(k, t) \rangle / \langle |E_{VV}(k, 0)|^2 \rangle \quad (7)$$

and

$$g_{VH}^{(1)}(k, t) = \langle E_{VH}^*(k, 0)E_{VH}(k, t) \rangle / \langle |E_{VH}(k, 0)|^2 \rangle. \quad (8)$$

Assuming independence of the translational and rotational dynamics, these equations can be written as [12],

$$g_{VV}^{(1)}(k, t) = [A + Bf_R(t)]f(k, t), \quad (9)$$

and

$$g_{VH}^{(1)}(k, t) = f_R(t)f(k, t), \quad (10)$$

where $f_R(t)$ and $f(k, t)$ are the dynamic correlation functions describing rotational and translational motion of single particles in the host matrix, respectively. Here $A = 45\alpha^2 / (45\alpha^2 + 4\beta^2)$, and $B = 4\beta^2 / (45\alpha^2 + 4\beta^2)$, where $\alpha = (1/3)(\alpha_{\parallel} + 2\alpha_{\perp})$, and $\beta = \alpha_{\parallel} - \alpha_{\perp}$ represent the isotropic and the anisotropic parts of the polarizability tensor. Thus, A and B depend only on intrinsic particle properties. In this work, those constants are determined by the light scattering from particles in water, using the condition $A+B=1$, and the ratio $(\alpha/\beta)^2 = (3\langle I_{VV} \rangle - 4\langle I_{VH} \rangle) / 45\langle I_{VH} \rangle$ [12, 13].

For non-interacting particles in a viscous fluid

$$f_R(t) = \exp(-6\Theta t), \quad (11)$$

and

$$f(k, t) = \exp(-k^2Dt). \quad (12)$$

Then,

$$g_{VH}^{(1)}(k, t) = \exp[-(6\Theta + k^2D)t] \equiv \exp(-t/\tau), \quad (13)$$

with

$$\tau^{-1} \equiv 6\Theta + k^2D. \quad (14)$$

Thus, for simple viscous systems, both diffusion constants D and Θ can be determined from $g_{VH}^{(1)}(k, t)$. Fig. 2 shows a plot of τ^{-1} vs. k^2 for a dilute aqueous suspension of the LC particles prepared as described in the previous section. As predicted by Eq. (13), anisotropic particles produce a finite value of the ordinate at $k = 0$, which gives the value of Θ . This term is produced by the anisotropy of the particles, and it is not present in isotropic particles. The radius for the LC particle calculated, from the slope, is 169.0 ± 3.7 nm, and calculated from the ordinate of origin is 166.0 ± 5.8 nm, which are equal within the experimental error.

In more complex cases, one needs to measure both $g_{VV}^{(1)}(k, t)$ and $g_{VH}^{(1)}(k, t)$ at the same scattering angle to disentangle the rotational from the translational correlation, *i.e.*, to get $f_R(t)$ and $f(k, t)$ separately. From Eqs. (9) and (10) we obtain

$$f_R(t) = \frac{Ag_{VH}^{(1)}(t)}{g_{VV}^{(1)}(t) - Bg_{VH}^{(1)}(t)}, \quad (15)$$

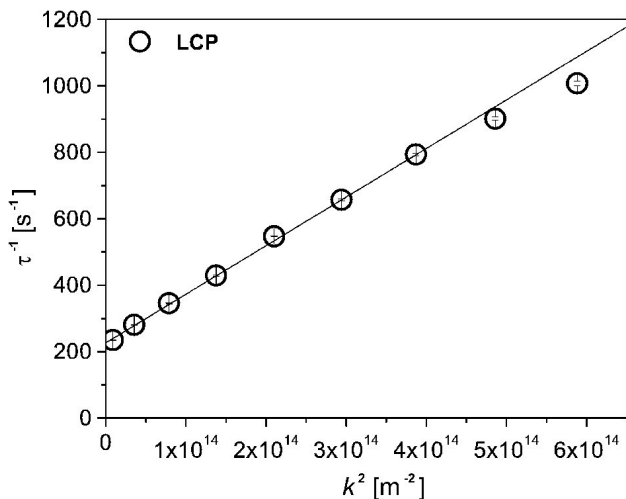


FIGURE 2. Decay constant τ^{-1} vs. k^2 measured for anisotropic LC particles immersed in water. Error bars are within the symbol size. The solid line is a linear fit of the experimental data to Eq. (14) from which we obtain $D = (1.463 \pm 0.032) \times 10^{-12} \text{ m}^2/\text{s}$ and $\Theta = 37.72 \pm 3.96 \text{ rad}^2/\text{s}$. The volume fraction of the LC particles is around 10^{-5} .

and

$$f(k, t) = \frac{1}{A} [g_{VV}^{(1)}(t) - Bg_{VH}^{(1)}(t)]. \quad (16)$$

The mean square rotational and translational displacements can then be obtained from these dynamic functions by using the Gaussian approximation, *i.e.*,

$$f(k, t) = \exp(-k^2 W(t)), \quad (17)$$

and

$$f_R(t) = \exp(-6\Omega(t)), \quad (18)$$

which are the generalization of Eqs. (11) and (12).

4. Results

Depolarized dynamic light scattering from optically anisotropic liquid crystal particles was measured for a variety of host media: water, polyacrylamide water solution without cross-linkers, and for 5 different fractional concentrations f_{bis} of bis-acrylamide from 0.25% to 1.25% in steps of .25%. In this range of cross-linker the system is below the sol-gel transition. Scattering from the host matrix is also observed, but the light intensity was always only 1-2% of that of the scattered light from the probes. Thus, the contribution from the matrix to the correlation functions is negligible. Figs. 3(a) and 4(a) show the intensity correlation functions measured for both scattering geometries VV and VH, respectively. In all the figures presented here the error bars are smaller than the symbols size, and they are omitted. Symbols correspond to different values of f_{bis} as indicated in the figures. The scattering angle was $\theta_s = 50^\circ$. Measurements at different scattering angles (data not shown) lead to similar

results. As shown in these figures, the intensity correlation functions satisfy the following limits: $g^{(2)}(k, t)$ approaches 2 as $t \rightarrow 0$, *i.e.*, $b = 1$ in Eq. (4). They also approach their asymptotic value of 1 at long times, which means a full relaxation of the correlation functions, *i.e.*, there are no frozen configurations of the colloidal particles in the scattering volume. Therefore, one can apply Eq. (4) to obtain the field correlation functions. Figs. 3(b) and 4(b) show the functions $g_{VV}^{(1)}(k, t)$ and $g_{VH}^{(1)}(k, t)$ corresponding to Figs. 3(a) and 4(a), respectively. As one can see here, the decay of both field correlation functions slow down appreciably upon the polymer formation in the system. The decaying time increases from few milliseconds in pure water to about 0.1 seconds in the polymer solution without cross-linker, with a further increase as f_{bis} increases. Thus, the presence of the polymer in the solution, even at $f_{bis} = 0$, has a strong effect on the particles dynamics.

A direct discussion of translational and rotational particle diffusion in these systems, from the correlation functions shown in Figs. 3 and 4, is difficult because this information is mixed in these quantities, see Eqs. (9) and (10). However, we can use Eqs. (15) and (16) to obtain separately the correlation functions associated to translational and rotational dynamics

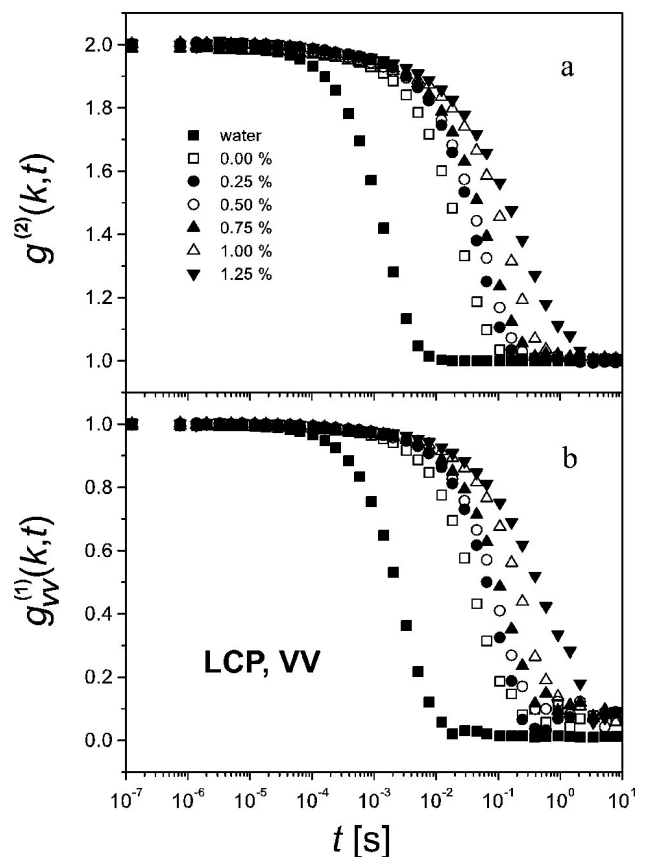


FIGURE 3. (a) Intensity and (b) field correlation functions of liquid crystal particles immersed in water (■), no cross-linked polymeric solution (□) and 5 polyacrylamide gels with different cross-linking fraction f_{bis} , measured in the VV geometry.

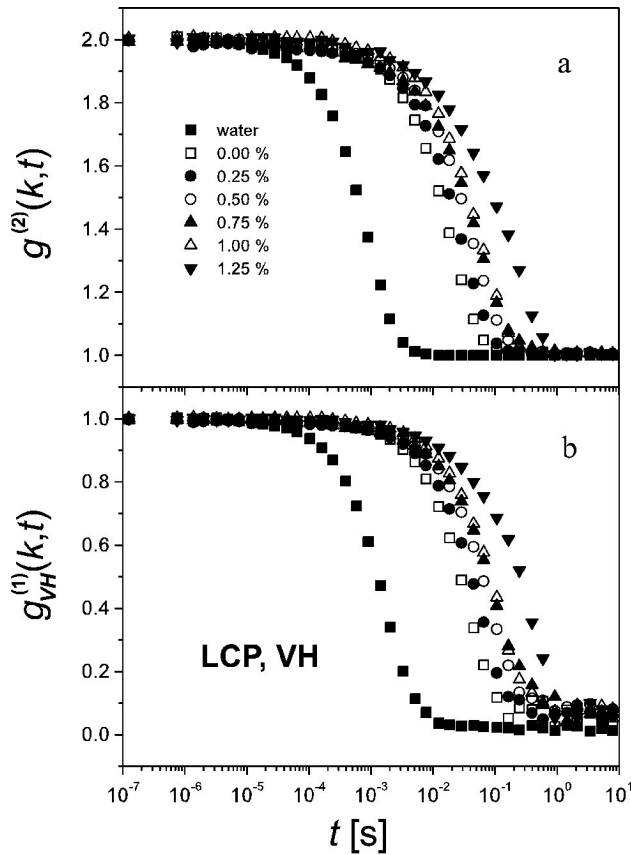


FIGURE 4. (a) Intensity and (b) field correlation functions of liquid crystal particles at the same conditions as in Fig. 3 but measured in the *VH* geometry.

of the particles, and Eqs. (17) and (18) to obtain the translational and rotational mean squared displacements. Figs. 5(a) and 5(b) show $W(t)$ and $\Omega(t)$, respectively, for the systems in Figs. (3) and (4). As one can see here, for the case of pure water, both mean squared displacements are linear functions of time in accord accordance with the Einstein's relations, Eqs. (1) and (2) for viscous fluids. However, in the systems with polymer both quantities curve downward continuously with time, even for $f_{bis} = 0$. A slow down of both diffusion modes could be understood in terms of a higher effective viscosity of the fluid. However, the curvature indicates a more complex (viscoelastic) response of the medium to the probes motion. The shape of $W(t)$ for $f_{bis}=1.25\%$ resembles the shape of the mean squared displacement of a Brownian particle harmonically bound to a spring of constant K , given by $W(t) = \delta r_0^2 [1 - \exp(-t/\tau)]$. Here $\delta r_0^2 = k_B T / K$, and $\tau = \zeta / 2K$. In this model, a restoring force bounds the particle to move around the center of the force with a characteristic angular frequency $\omega = (\zeta / 2m\tau)^{1/2}$, and $W(t)$ reaches an asymptotic value of δr_0^2 for $t \gg \tau$. In the systems studied in the present work, the particles are not bound to a fix configuration, but they diffuse through, *i.e.*, both mean squared displacements bend, but do not level off in any of systems studied, even for the higher cross-linker fraction $f_{bis} = 1.25\%$. Thus, the model of the harmonically bound Brownian parti-

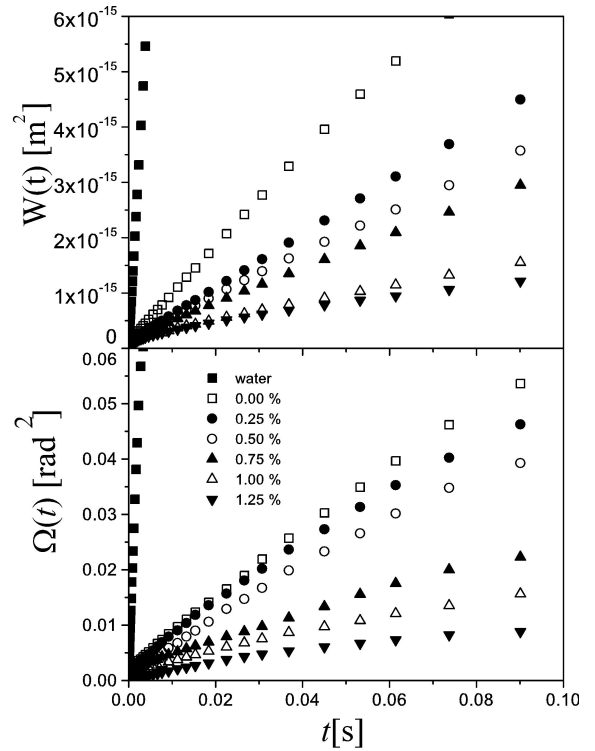


FIGURE 5. (a) Translational and (b) rotational mean squared displacements of liquid crystal particles in the systems of Figs. 3 and 4.

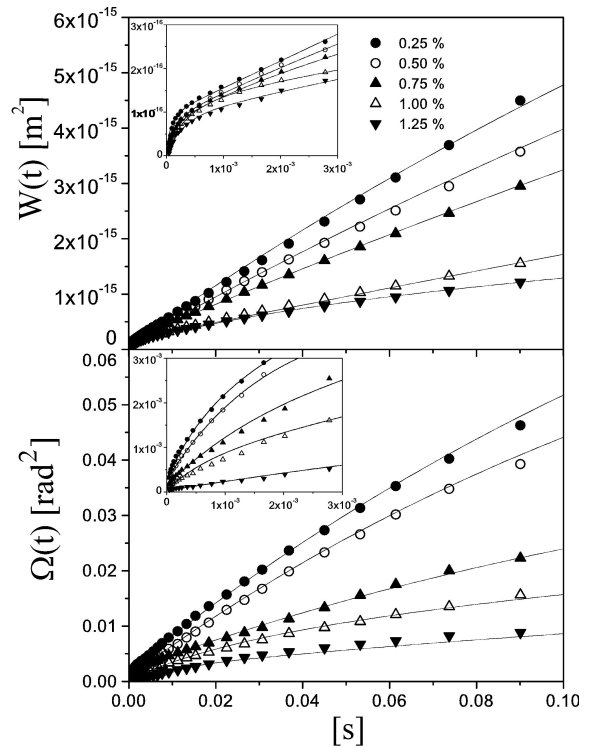


FIGURE 6. (a) Translational and (b) rotational mean squared displacements of liquid crystal particles for five gels with different cross-linking fraction f_{bis} (symbols) and the fits (solid lines) of the experimental data to Eqs. (19) and (20) with N between 3 and 5.

cle can not be applied directly to our case. Nevertheless, one can still consider the particles to be locally subjected to a superposition of weak restoring forces and torques of different characteristic frequencies $\omega_i = (\zeta/2m\tau_i)^{1/2}$, *i.e.*,

$$W(t) = \delta r_0^2 \left(1 - \sum_{j=1}^N c_j e^{-t/\tau_j} \right), \quad (19)$$

where N is the number of modes, and c_j is the amplitude of the j th translational mode which satisfy the condition $\sum_j c_j = 1$. We can also propose the extension of this model to describe rotational diffusion, *i.e.*,

$$\Omega(t) = \hat{n}_0^2 \left(1 - \sum_{j=1}^N c_j^n e^{-t/\tau_j^n} \right), \quad (20)$$

where N , τ_j^n , and c_j^n have the same meaning as in the previous case, with the condition $\sum_j c_j^n = 1$.

Fits of the experimental data for $W(t)$ and $\Omega(t)$ to Eqs. (19) and (20), respectively, are shown in Fig. 6 (solid lines). The insets show a closeup of the dynamics at the short time scale. Here one can see in more detail the continuous curvature of both mean squared displacements, and the fits to the extended harmonic model. For the lower concentrations of cross-linker we need $N = 3$ to have a good fit to the experimental data in the whole time regime. As we increase

the cross-linker fraction, we require to increase the number of modes up to $N = 5$ for $f_{bis} = 1.25\%$. Although a good quality fitting to the experimental data can be achieved using other functional forms with the number of free parameters used here, we consider that the use of Eqs. (19) and (20) provide us with a simple physical model where the free parameters can be related to physical properties of the system; for instance, the time decay constants could be related to characteristic frequencies of the viscoelastic host medium.

This work presents a methodology to study simultaneously the translational and rotational motion of spherical colloidal probes in weak gels with viscoelastic properties. As shown here, both diffusion modes are sensible to the mechanical properties of the host medium. Thus, both dynamics can give independent and complementary information, and open the possibility to study a number of different media where rotational motion can be applied as a novel and useful tool.

Acknowledgments

Work partially supported by the Consejo Nacional de Ciencia y Tecnología, México, Grants G29589E and ER026 Materiales Biomoleculares, and by the Instituto Mexicano del Petróleo, México, Grant FIES-98-101-I.

-
1. S. Chandrasekhar, *Rev. Mod. Phys.* **15** (1943) 1.
 2. J.D. Ferry, *Viscoelastic Properties of Polymer* (Clarendon Press, Oxford, 1949).
 3. J.K.G. Dhont, *An Introduction to Dynamics of Colloids* (Elsevier Science, Amsterdam, 1996).
 4. P. N. Pusey, in *Liquids, Freezing and Glass Transition*, edited by J.P. Hansen, D. Levesque, and J. Zinn-Justin (Elsevier, 1991).
 5. T.G. Mason and D.A. Weitz, *Phys. Rev. Lett.* **74** (1995) 1250.
 6. A.W.C. Lau, B.D. Hoffman, A. Davies, J.C. Crocker, and T.C. Lubensky, *Phys. Rev. Lett.* **91** (2003) 198101.
 7. G. Popescu, A. Dogariu, and R. Rajagopalan, *Phys. Rev. E* **65** (2002) 041504.
 8. M.L. Gardel, M.T. Valentine, J.C. Crocker, A.R. Bausch, and D.A. Weitz, *Phys. Rev. Lett.* **91** (2003) 158302.
 9. A. Mertelj, J.L. Arauz-Lara, G. Maret, T. Gisler, and H. Stark, *Europhys. Lett.* **59** (2002) 337.
 10. J. Bibette, *J. Coll. Int. Sci.* **147** (1991) 474.
 11. I. Nishio, J.C. Reina, and R. Bansil, *Phys. Rev. Lett.* **59** (1987) 684.
 12. B.J. Berne and R. Pecora, *Dynamic Light Scattering: With Applications to Chemistry, Biology and Physics* (John Wiley, New York, 1976).
 13. V. Degiorgio, R. Piazza, and T. Bellini, *Adv. Coll. Int. Sci.* **48** (1994) 61.